Materials Sciences and Applications, 2016, 7, 848-862
http://www.scirp.org/journal/msa
ISSN Online: 2153-1188
ISSN Print: 2153-117X

Experimental Study of Acoustic Noise Correlation Technique for Passive Monitoring of Rails

Laïd Sadoudi, Emmanuel Moulin, Jamal Assaad, Farouk Benmeddour, Michaël Bocquet, Yassin El Hillali

Département OAE, Université de Valenciennes et du Hainaut Cambrésis, Valenciennes, France
Email: laid.sadoudi@gmail.com

How to cite this paper: Sadoudi, L., Moulin, E., Assaad, J., Benmeddour, F., Bocquet, M. and El Hillali, Y. (2016) Experimental Study of Acoustic Noise Correlation Technique for Passive Monitoring of Rails. *Materials Sciences and Applications*, **7**, 848-862.
http://dx.doi.org/10.4236/msa.2016.712065

Received: October 16, 2016
Accepted: December 10, 2016
Published: December 13, 2016

Abstract

The work presented in this paper aims at investigating the ability of acoustic noise correlation technique for railway infrastructure health monitoring. The principle of this technique is based on impulse responses reconstruction by correlation of random noise propagated in the medium. Since wheel-rail interaction constitutes a source of such noise, correlation technique could be convenient for detection of rail defects using only passive sensors. Experiments have been carried out on a 2 m-long rail sample. Acoustic noise is generated in the sample at several positions. Direct comparison between an active emission-reception response and the estimated noise correlation function has confirmed the validity of the equivalence relation between them. The quality of the reconstruction is shown to be strongly related to the spatial distribution of the noise sources. High sensitivity of the noise-correlation functions to a local defect on the rail is also demonstrated. However, interpretation of the defect signature is more ambiguous than when using classical active responses. Application of a spatiotemporal Fourier transform on data recorded with variable sensor-defect distances has allowed overcoming this ambiguity.

Keywords

Acoustic Noise Correlation, Signal Processing, Passive Green's Function Reconstruction, Non-Destructive Testing (NDT), Structural Health Monitoring (SHM), Rail Monitoring

1. Introduction

Transportation is an activity that involves significant risks due to the displacement speed of vehicles. Materials used in this context are exposed to severe operating condi-

tions leading to premature wear, deformations, and failures of all kinds. This obviously requires serious and costly maintenance strategies.

In the railway industry, in particular, technicians walk along the rail tracks to detect any defects or missing component [1] [2]. Automated vision systems have been developed to eliminate or minimize the visual inspections by humans, but still detection is limited to visible anomalies. Existing technologies for finer local inspection and detection of early damage include: eddy current [3], fiber optic sensors [4] [5], and naturally ultrasound NDT using either contact or contact-less acoustic sensors [6] [7] [8] [9] [10]. Though efficient, these methods ordinarily require planning interventions depending on traffic. This can lead to disruption of rail services and even periodic shutdown, meaning significant costs for railway companies. Other important aspects are implicated: reliability and security. Indeed, it is possible that unforeseen technical problems appear between two planned inspections with at the least enormously costly and, possibly, dramatic consequences.

For these reasons, the concept of intelligent infrastructure [11] [12] with continuous monitoring capabilities is currently receiving growing interest. Trends for future track monitoring systems are either SHM systems based on integrated sensors or systems embarked on regular commercial trains. In either cases, non-intrusiveness and low-consumption will be major requirements.

Recent theoretical and experimental works have demonstrated the potential of an original ultrasound technique relying on the correlation of non-coherent acoustic fields [13] [14] [15] [16]. Based on passive Green's function reconstruction [17], the principle is that such fields, ordinarily considered as noise in conventional NDT applications, can be judiciously exploited to estimate the response between two measurement points without the need for an active ultrasound source at one of these points. This technique could thus offer the opportunity of a real-time monitoring, in all situations where an ambient acoustic noise exists. The advantage of using only passive sensors instead of ultrasound emitter-receivers resides in limited necessary hardware and lower consumption of the system.

The objective of this work is to study the feasibility of such acoustic noise correlation technique in the railway field. When a train is moving, dynamical mechanical interactions between the rail and the train wheels will naturally generate guided elastic waves in the rail. The presence of these waves, which can be considered as an ambient noise since their excitation is uncontrolled, makes indeed the railway application eligible for this correlation technique. We present here a first laboratory study aiming at assessing the applicability of the concept in this particular context of a one-dimensional elastic waveguide.

First, the degree of validity of the cross correlation technique for passive reconstruction of the Green's function (active response) is experimentally tested on an actual rail sample. Ambient noise insonification is simulated by means of piezoelectric patches coupled to the sample and fed with wideband electrical noise. Finally the noise-correlation functions are applied to the detection of a local heterogeneity (defect) in the rail

sample. The obtained results show a clear sensitivity to the defect in the considered experimental conditions. Furthermore, it is shown that introduction of spatiotemporal information through the use of several defect-sensor distances and comparison to the numerical dispersion curves allow improved characterization of the defect signature retrieved by the noise correlation process.

2. Experimental Setup

Theoretical and experimental studies in several areas [16]-[21], have shown the existence of a relationship between the Green's function (acoustic impulse response) between two measurement points and the cross-correlation of noise signals recorded at these points.

This section presents an experimental study about the effective reconstruction of the active response from the cross-correlation function of noise fields.

The experiments are performed on a 2~m-long rail sample with a cross section shown in **Figure 1**.

2.1. Active Response Measurement

Two PZ27-piezoelectric transducers of 27~mm radius and 0.43~mm thickness have been glued on the rail foot at positions A and B. A function generator is used to generate the excitation signal at transducer A and the signal received at transducer B is acquired using an oscilloscope synchronized with the function generator and linked to a computer through a GPIB interface (**Figure 2(a)**).

The transmitter (A) is excited with an electric signal $s_0(t)$ corresponding to a one-cycle sine pulse train at 50 kHz and with an amplitude of 10 V. The measured signals are averaged over 128 acquisitions in order to improve the signal to noise ratio (SNR). **Figure 3** shows a signal measured in this configuration. It is a typical reverberated signal consisting of the direct propagation from A to B and a large number of multiple reflexions, scattering, mode conversions on the domain boundaries (edges of the rail) and possible inhomogeneities. After 80 ms, this signal is completely attenuated.

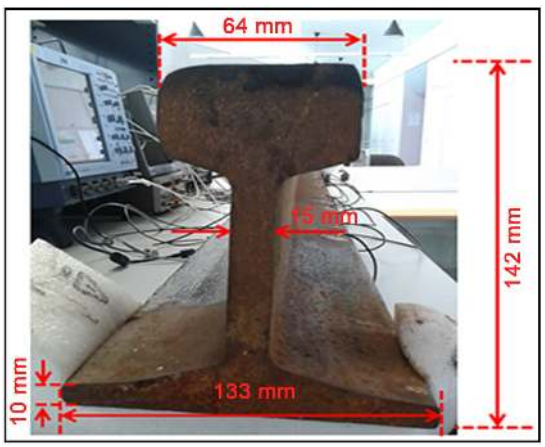

Figure 1. Picture of the cross section of the rail sample used in this study (figure caption).

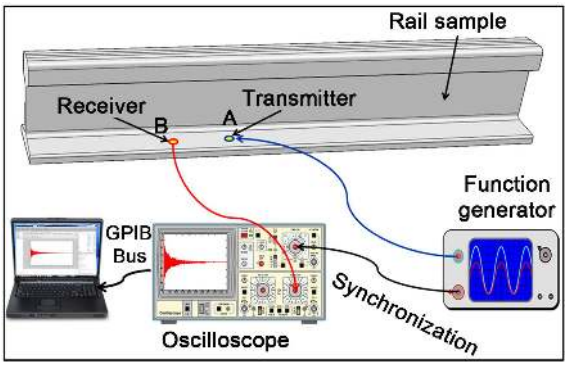

(a)

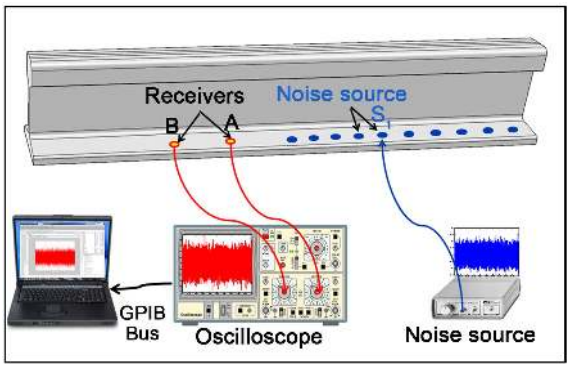

(b)

Figure 2. Experimental setup. (a) Active experiment; (b) Noise-correlation experiment.

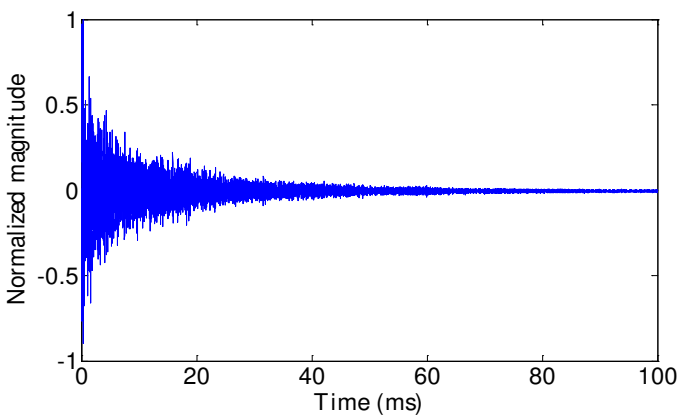

Figure 3. Typical response measured by the receiver at B when the transducer A is excited by a one-cycle pulse train at 50 kHz.

2.2. Noise Correlation Measurement

For the noise-correlation experiment, the function generator is removed and both transducers A and B are used as receivers. In order to generate acoustic noise in the rail, ten piezoelectric transducers of the same type as in the previous experiment and glued on the rail foot at positions Si are successively fed by an electrical noise generator (Figure 2(b)).

The noise correlation function R_{AB} is experimentally estimated from finite-time correlations averaged over a number M of acquisitions. More precisely, an estimator of the correlation function corresponding to each noise source is defined as

$$\tilde{R}_{AB}^{(n)}(t)=\frac{1}{M}\sum_{m=1}^{M}\int_{0}^{T}S_{A}^{(m,n)}(\tau)S_{B}^{(m,n)}(t+\tau)\mathrm{d}\tau, \tag{1}$$

where T is the recorded signal duration and $S_{X}^{(m,n)}(t)$ is the signal recorded at X in the m^{th} acquisition of the measurements performed when the n^{th} noise source S_n is active.

Then, the global correlation estimator for the case with the N noise sources is simply defined as

$$\tilde{R}_{AB}(t)=\sum_{n=1}^{N}\tilde{R}_{AB}^{(n)}(t) \tag{2}$$

The study will focus on the influence of the number of acquisitions M and the number of noise sources N on the convergence of the correlation estimations towards the active response.

Considering that the signal duration in the considered frequency range is about 80 ms, as seen on Figure 3, a record duration T = 100 ms is chosen.

Figure 4(a) shows the first wave packets of the positive-time part of the estimated cross-correlation functions $\tilde{R}_{AB}^{(1)}(t)$ obtained with different values of the number of

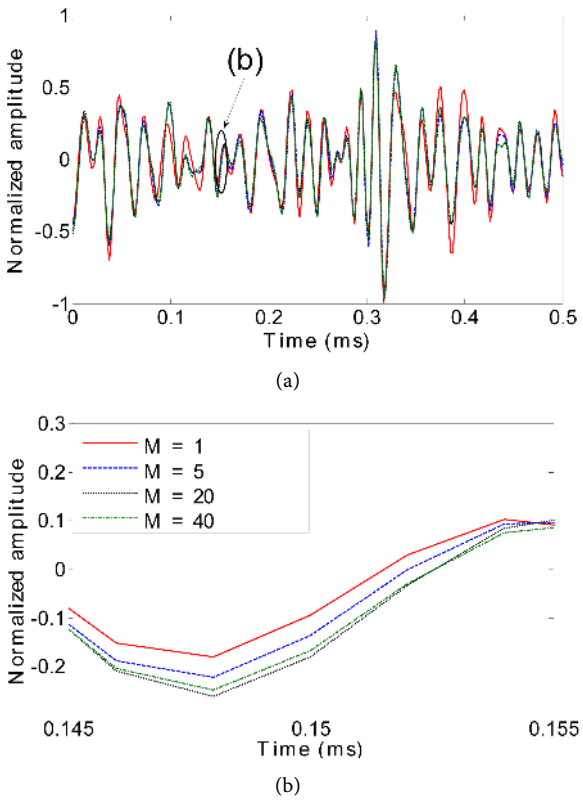

Figure 4. Influence of the number of acquisitions (M) on the estimated correlation. (a) First wave packets of $\tilde{R}_{AB}^{(1)}(t)$; (b) Zoom on the waveform part circled on (a).

acquisitions M, and a single noise-source position ($N = 1$). Since the absolute amplitudes of the presented waveforms are useless here, they have been systematically normalized with respect to their maximum values. For better visualization, a zoom on an arbitrary part of the waveforms is presented on **Figure 4(b)**. It appears that the estimated correlation begins to converge when averaging over 20 acquisitions or more. This is regarding to the Equation (1). The lager the M, the better the convergence. Therefore, a value of $M = 20$ will be retained as a satisfying compromise between estimation accuracy and the required time for measurement and computation.

The next step aims to determine the number of source positions to converge towards the active response. Indeed, the diffuse field assumption is a necessary condition for this convergence. Multiplicating the number of sources distributed on the medium will help to get closer to this theoretical condition and subsequently ensure a better convergence. It is known that the temporal symmetry of the noise correlation functions is a good indicator of the quality of this convergence. The reason for that is the acoustic reciprocity principle [22], which implies that the Green's function from A to B is the same as the one from B to A. Therefore the symmetry of the estimated correlation functions $\tilde{R}_{AB}(t)$ for different values of the number N of noise sources will be checked. To that end, the positive-time and negative-time parts of $\tilde{R}_{AB}^{(1)}(t)$ are compared on **Figures 5**.

For $N = 2$, **Figure 5(a)**, it is clear that the positive-time and negative-time parts of the estimated cross-correlation differ significantly. For $N = 5$, **Figure 5(b)**, a better agreement between both parts is observed and, finally for $N = 10$, **Figure 5(c)**, a clear similarity is obtained. Thus, in that case, the estimated cross-correlation function satisfies the reciprocity principle, as does the active response s_{AB}. It will be verified now that this case corresponds to a satisfying comparison between both.

The aim here is to compare this passively obtained response to the active signal s_{AB}. We define the quantity

$$\tilde{D}_{AB}^{+}(t) = \frac{\mathrm{d}\tilde{R}_{AB}^{+}(t)}{\mathrm{d}t} \otimes s_0(t) \tag{3}$$

where s_0 is the excitation signal used in the active experiment, and $\tilde{R}_{AB}^{+}$ is the positive-time part of the correlation estimator.

In **Figure 6(a)**, $\tilde{D}_{AB}^{+}(t)$ obtained with the 10 noise sources is compared to the active response $s_{AB}(t)$. Here again, the presented waveforms have been normalized with respect to their maximum values. Wave-packets appear correctly reconstructed but a clear phase shift is observed. This phase shift can be interpreted as the effect of the (unknown) transduction impulse response $c(t)$ (electro-mechanical and reciprocal conversions of the transducers). An empirical compensation of this phase shift, as shown in **Figure 6(a)** confirms that the noise-correlation response $\tilde{D}_{AB}^{+}(t)$ constitutes indeed a very good estimation (or "reconstruction") of the active response. The slight differences between both responses can be interpreted as the reconstruction error, also referred to as "correlation residue".

In the remainder of this paper, the cross-correlation functions will thus be estimated using $N = 10$ noise source positions and $M = 20$ acquisitions for each position.

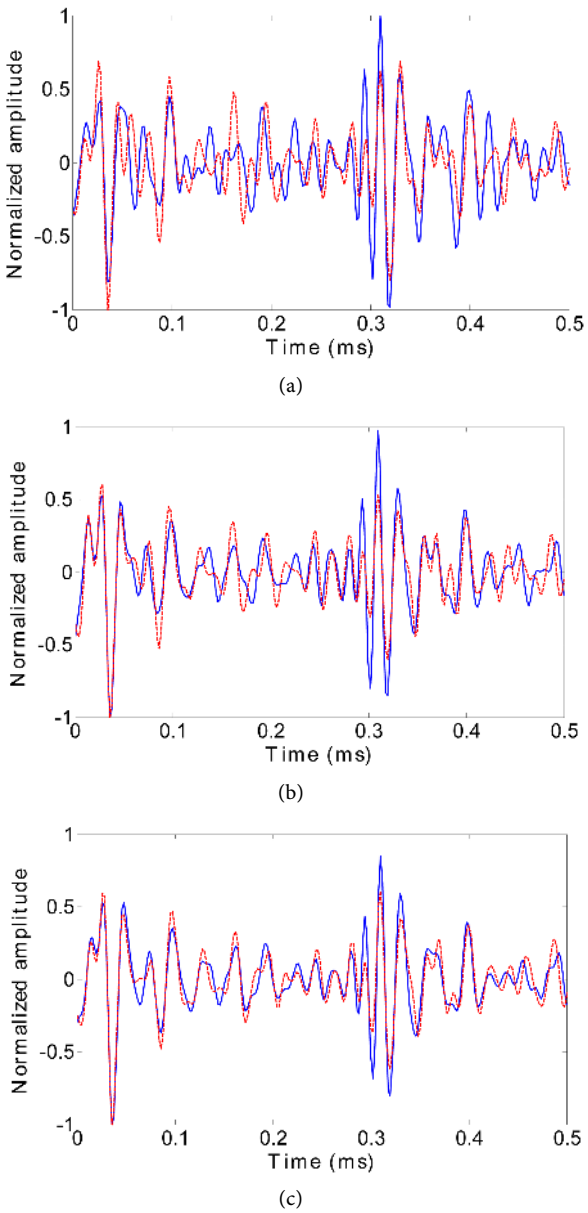

Figure 5. Comparison of the positive-time (——) and negative-time (----) parts of the estimated cross-correlation for different values of the number of sources positions: (a) $N = 2$; (b) $N = 5$ and (c) $N = 10$.

3. Application to Defect Detection

This section aims to demonstrate the applicability of the estimated noise correlation function to detect a defect in the rail sample. Indeed, the occurrence of any local change in the medium will introduce reflection and transmission phenomena in the propagation. This will induce a modification of the active response between the two transducers. Experimental observation of such modification means detection of the defect. The efficient reconstruction of the active response shown in the previous section indicates that defect detection should also be achievable using noise correlation.

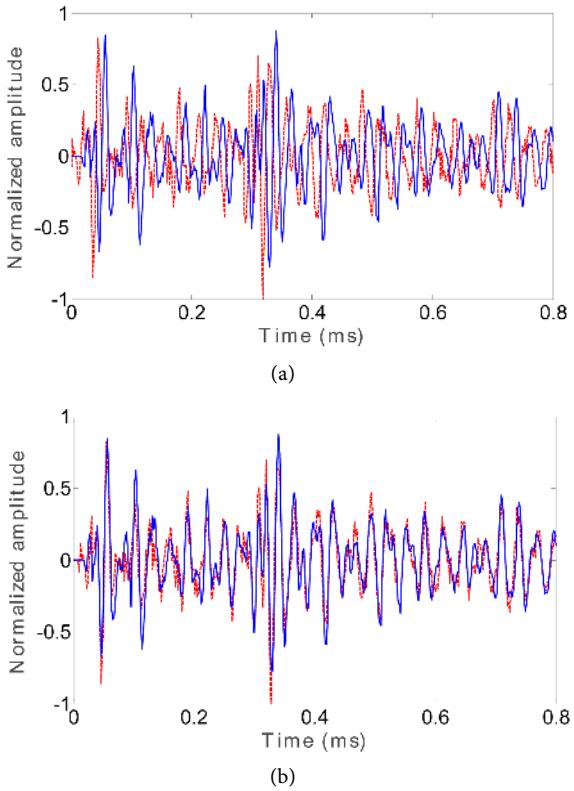

Figure 6. Comparison between the measured active response $s_{AB}(t)$ (—) and $\tilde{D}^{+}_{AB}(t)$ obtained from the estimated noise-correlation following Equation (3) for $N = 10$ noise sources (----). (a) Raw waveforms; (b) Waveforms with phase shift compensation.

3.1. Sensitivity to a Local Defect

The experimental setup used to perform the measurements presented here is the same as in the previous section (**Figure 2**). In order to allow repeatable and non-destructive experiments, we used a local change that did not damage irreversibly the rail sample. Therefore what will be referred to as the "defect" in the remaining of this paper is a local pressure applied to the rail foot by a locking plier as shown in **Figure 7**. Such static mechanical action will modify locally the guided wave propagation sufficiently to introduce reflection and transmission phenomena comparable to the effect of an actual damage such as a hole or a crack. This defect is placed at a distance $d = 5$ cm from the measurement point B as shown in **Figure 8**.

Waveform differencing (also known as baseline subtraction) is used throughout the experimental measurements presented in this section. Therefore, active and noise-correlation measurements are first performed without defect. The obtained signals constitute the reference (or baseline) waveforms $s^{\text{ref}}_{AB}(t)$ and $\tilde{R}^{\text{ref}}_{AB}(t)$ (or equivalently $\tilde{D}^{\text{ref}}_{AB}(t)$), respectively. Second, the same measurements are performed with the presence of the defect and corresponding waveforms are noted $s^{\text{def}}_{AB}(t)$ and $\tilde{R}^{\text{def}}_{AB}(t)$. Finally, the reference waveforms are subtracted from those obtained with the defect, yielding

$$\Delta s_{AB}(t) = s^{\text{def}}_{AB}(t) - s^{\text{ref}}_{AB}(t) \tag{4}$$

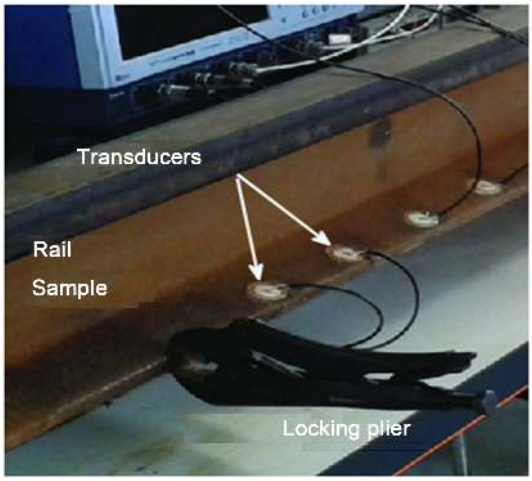

Figure 7. Picture of defect simulation in the rail sample using locking plier.

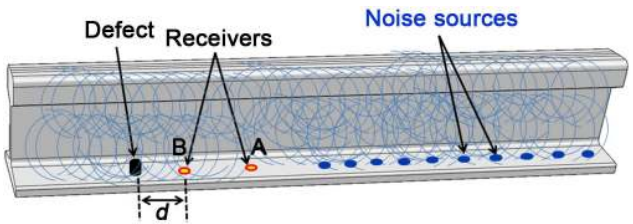

Figure 8. Defect detection by cross-correlation of noise fields between two measurement points of the rail.

the differential active response, and

$$\Delta\tilde{R}_{AB}(t) = \tilde{R}_{AB}^{\text{def}}(t) - \tilde{R}_{AB}^{\text{ref}}(t) \tag{5}$$

the differential noise-correlation response (or again equivalently $\Delta\tilde{D}_{AB}(t) = \tilde{D}_{AB}^{\text{def}}(t) - \tilde{D}_{AB}^{\text{ref}}(t)$).

These differential waveforms are representative of the defect signature. The early wave-packets of the measured Δs_{AB}, normalized with respect to the maximum value of s_{AB}^{ref}, are shown in **Figure 9(a)**. The first wave packet (beginning just before 0.1 ms) corresponds to the first reflection on the defect, whereas the other ones correspond to combinations of transmitted or reflected waveforms on the defect and reflections at the rail sample extremities.

The differential noise-correlation response $\Delta\tilde{D}_{AB}$, obtained with the experimental parameters previously determined ($M = 20$, $N = 10$) and normalized with respect to $\tilde{R}_{AB}^{\text{ref}}$, is shown in **Figure 9(b)**. Comparing **Figure 9(a)** and **Figure 9(b)**, some similarities between both waveforms are visible. Yet, significant differences are also noticeable. In particular, a first wave-packet of significant amplitude is apparent between 0 and 0.08 ms in the differential noise-correlation response. This wave-packet makes the one associated to the reflection on the defect far less evident than it is in the active differential response. This can be explained by the fact that the reconstruction of the active responses by the noise correlation process relies on all reverberated wave-packets. Since

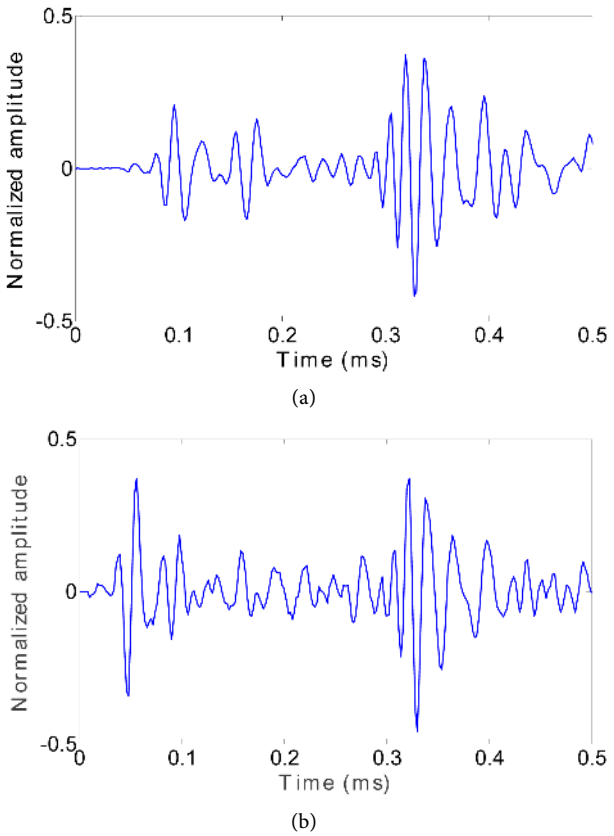

Figure 9. Sensitivity to a defect: (a) Active detection $\Delta s_{AB}(t)$; (b) Noise correlation detection $\Delta\tilde{D}^{+}_{AB}(t)$.

the introduction of any local change in the medium will both modify all wave-packets going through it and add reflected ones, it will entail changes in the reconstruction process itself. This means that in $\Delta\tilde{D}_{AB}$, the identifiable defect signature (temporally related to the defect position, as in Δs_{AB}) will be mixed with differences in the correlation residues that have no particular localization in time.

Though this shows obviously that noise correlation is clearly sensitive to a change in the medium, the difficulty to relate the differential noise-correlation response to the position might be a problem. Indeed, the need to discriminate a local defect from a change in the boundary conditions at the rail extremities or a global material variation such as induced by temperature changes or other effects might be crucial in a realistic situation.

Therefore, it is important to be able to extract some information coherently related to the defect position. To that end, we propose in the next section an experiment based on several acquisitions where multiple defect-sensor distances are considered.

3.2. Extraction of Coherent Information

A rather natural way to exhibit information related to the position of either a source or a scatterer is to interrogate several propagation distances. Therefore, the same kind of

measurements as in the previous paragraph will be performed here, but with varying defect-transducer distances. For practical reasons, instead of moving the transducers or using several ones at different positions (as would be logical in a real SHM situation), we will move the local "defect" constituted by the locking plier pressure.

The transducers used are the same as previously (A and B) and the noise-correlation parameters are kept unchanged (N = 10 source positions, M = 20 acquisitions per source). A set of active signals and correlation responses for 24 defect positions are recorded. The positions are defined by $d_i = d + (i-1)\Delta x$, where d_i is the i^{th} distance between defect and transducer B (see Figure 10). The initial distance d is 5 cm and the displacement step Δx is 1 cm.

By subtracting here again the reference signal and correlation responses without defect to the newly recorded waveforms, 24 differential active responses $\Delta s_{AB}^{\text{def},i}(t)$ and 24 differential noise-correlation responses $\Delta R_{AB}^{\text{def},i}(t)$ are obtained. The upper script i indicates the defect position index. These waveforms are presented in Figure 11(a) and Figure 11(b), respectively, in the form of spatial-temporal information. Interpretation of Figure 11(a) is straightforward: the first wave-packet corresponding to the reflection on the defect has a propagation time proportional to the distance d_i, which manifests itself by a neat slope (between approximately 0.1 ms at 5 cm and 0.25 ms at 29 cm) on the spatial-temporal image.

Figure 11(b) is visually noisier. The first wave-packet (before 0.05 ms) does not apparently propagate and, though it is evidently related to the defect's presence, it is independent from its position. This confirms the remark made previously about Figure 9(b). A propagative component is also visible, though not very clearly, with the same slope as in the actively-obtained image. Note that we have represented here $\Delta\tilde{R}_{AB}$ directly and not the time-derivate and convoluted version $\Delta\tilde{D}_{AB}$, which is only useful for precise quantitative comparisons with the active responses. For identification of the propagative component, $\Delta\tilde{R}_{AB}$ is as suitable as $\Delta\tilde{D}_{AB}$.

In order to better emphasize the presence of this propagative component related to the first reflection on the defect, a two-dimensional (spatial-temporal) Fourier transform (2D-FT) has been applied. This leads to a representation in the frequency-wavenumber domain that can be directly compared to the dispersion curves of elastic guided waves in the rail.

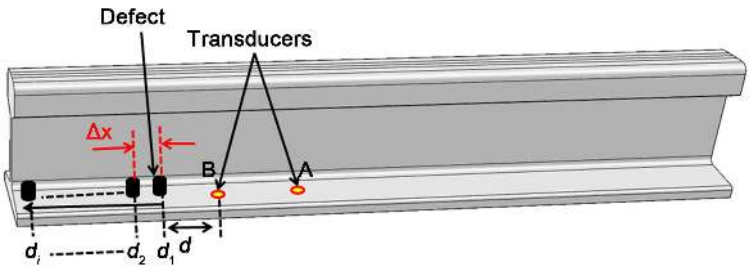

Figure 10. Description of experimental setup for measurement with variable receiver-defect distances.

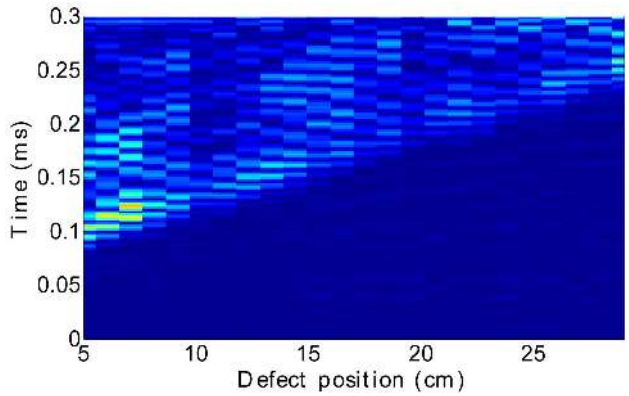

(a)

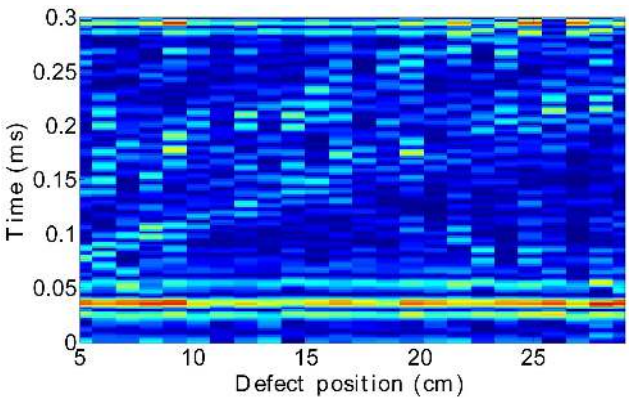

(b)

Figure 11. Spatio-temporal representations as a function of the defect position: (a) differential active responses $\Delta s_{AB}(t)$, and (b) differential noise-correlation estimations $\Delta\tilde{R}_{AB}(t)$ with $M = 20$ and $N = 10$.

Figure 12(a) shows the 2D-FT of the differential active responses. The dispersion curves, computed using the Semi-Analytical Finite Element (SAFE) technique [23], have been superimposed for easier interpretation of the frequency-wavenumber image. The strongest propagative component (corresponding to the slope visible on **Figure 11(a)** and commented above) appears to match with the guided mode of highest wavenumber. Logically, the mode shape of this mode happens to be essentially concentrated in the rail foot, where the transducers and the defect are located.

The same kind of interpretation can be made for **Figure 12(b)**, where the 2D-FT image of the differential noise-correlation responses is compared to the same dispersion curves. First, it can be observed that high-amplitude spots are present around zero wavenumber. This corresponds to the non-propagative components resulting from the correlation residues as discussed above. However, the propagative component related to the same guided mode as in the active experiment is also clearly visible.

This confirms that the wave-defect interaction process, ordinarily exhibited by actively launching incident waves, manifests itself in the same way in noise-correlation measurements. This means in particular that information related to the defect-sensor

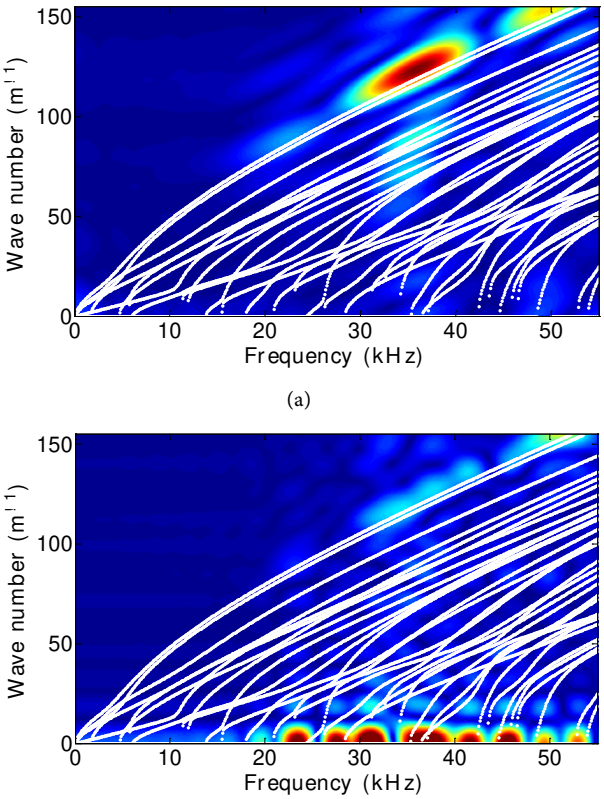

Figure 12. Spatio-temporal Fourier transforms (2D-FT) and comparison with numerical dispersion curves. (a) 2D-FT of Δs_{AB}; (b) 2D-FT of $\Delta\tilde{R}_{AB}$.

distances (and consequently to the defect position) is effectively present in, and eventually extractible from, an ambient noise.

4. Conclusions

This paper presents a preliminary study for the application of noise correlation technique to reconstruct the active response between two acoustic receivers in a rail sample. It is shown that a good quality of reconstruction is achieved, providing that the number of acquisitions and the number of distributed noise sources are sufficient. Then, baseline subtraction (waveform difference between the reference state and the state with defect) allows isolating the effect of a local defect on the estimated noise correlation functions. This effect is shown to consist of a contribution related to the defect position and a second one corresponding to the difference of the reconstruction errors between the states with and without defect. The use of several sensor-defect distances allows discriminating the first contribution in the form of a propagative component, whose characteristics match a waveguide mode concentrated in the rail foot, where the defect stands. Since this propagative component contains information related to the defect position, a localization of the defect from a set of passive sensors might be envisaged in future works. Testing with actual ambient noise (wheel-rail interaction) is also in pros-

pect.

If confirmed in more realistic field conditions, it is thought that these first encouraging results might open the way towards a passive, low-consumption, possibly non-intrusive and wireless system for rail monitoring.

Acknowledgements

The authors would like to thank the Region Nord-Pas de Calais and the Competitiveness Cluster i-Trans for their financial support.

References

[1] Camargo, L.F.M., Resendiz, E., Hart, J., Edwards, J.R., Ahuja, N. and Barkan, C.P.L. (2011) Machine Vision Inspection of Railroad Track. *USDOT Region V Regional University Transportation Center Final Report*, NEXTRANS Project No. 0281Y02.

[2] Marino, F., Distante, A., Mazzeo, P.L. and Stella, E. (2007) A Real-Time Visual Inspection System for Railway Maintenance: Automatic Hexagonal-Headed Bolts Detection. *IEEE Transactions on Systems, Man, and Cybernetics, Part C: Applications and Reviews*, **37**, 418-428. https://doi.org/10.1109/TSMCC.2007.893278

[3] Heckel, T., Thomas, H.M., Kreutzbruck, M. and Rühe, S. (2009) High Speed Non-Destructive Rail Testing with Advanced Ultrasound and Eddy-Current Testing Techniques. *Indian National Seminar & Exhibition on Non-Destructive Evaluation*, NDE, 10-12 December 2009.

[4] Zeni, L., Minardo, A., Porcaro, G., Giannetta, D. and Bernini, R. (2013) Monitoring Railways with Optical Fibers. SPIE Newsroom, Bellingham.

[5] Minardo, A., Porcaro, G., Giannetta, D., Bernini, R. and Zeni, L. (2013) Real-Time Monitoring of Railway Traffic Using Slope-Assisted Brillouin Distributed Sensors. *Journal of Applied Optics*, **52**, 3770-3776. https://doi.org/10.1364/AO.52.003770

[6] Frankenstein, B., Augustin, J., Hentschel, D., Schubert, F., Köhler, B. and Meyendorf, N. (2007) Acoustic Techniques for Structural Health Monitoring. *Review of Progress in Quantitative Nondestructive Evaluation*, **27B**, 1428-1435.

[7] Peng, C., Gao, X., Wang, L., Zhang, Y., Peng, J. and Yang, K. (2011) Ultrasonic Signal Multiplex Technology for Dynamic Wheelset Defect Detection System. 2011 *International Conference on Information Technology, Computer Engineering and Management Sciences* (*ICM*), Nanjing, 24-25 September 2011, 260-262. https://doi.org/10.1109/ICM.2011.232

[8] Willems, H., Jaskolla, B., Sickinger, T., Barbian, O.A. and Niese, F. (2010) Advanced Possibilities for Corrosion Inspection of Gas Pipelines Using EMAT-Technology. 10*th European Conference on Non-Destructive Testing*, Moskau, 7-11 June 2010, CD-ROM.

[9] Zhou, Z., Zhang, H. and Wei, D. (2010) Application of Pulse Compression Technique in Air-Coupled Ultrasonicnon-Destructive Testing on Composite Material. 10*th European Conference on Non-Destructive Testing*, Moskau, 7-11 June 2010.

[10] Blouin, A., Lvesque, D., Kruger, S. and Monchalin, J. (2009) Laser Ultrasonics for NDE in the Automotive Industry. *6th International Workshop for Signal Processing for NDE of Materials*, London Ontario, Canada, 25-27 August 2009.

[11] Ollier, B. (2006) Intelligent Infrastructure—The Business Challenge. *Proceedings of IET International Conference on Railway Condition Monitoring*, Birmingham, 29-30 November 2006, 1-6. https://doi.org/10.1049/ic:20060034

[12] Da Costa Marques Pimentel, R., *et al*. (2008) Hybrid Fiber-Optic/Electrical Measurement System for Characterization of Railway Traffic and Its Effects on a Short Span Bridge. *IEEE Sensors Journal*, **8**, 1243-1249. https://doi.org/10.1109/JSEN.2008.926519

[13] Larose, E., Lobkis, O.I. and Weaver, L. (2006) Passive Correlation Imaging of a Buried Scatterer. *The Journal of the Acoustical Society of America*, **119**, 3549-3552. https://doi.org/10.1121/1.2200049

[14] Sabra, K.G., *et al*. (2007) Using Cross Correlations of Turbulent Flow-Induced Ambient Vibrations to Estimate the Structural Impulse Response. Application to Structural Health Monitoring. *The Journal of the Acoustical Society of America*, **121**, 1987-1995.

[15] Moulin, E., Leyla, N.A., Assad, J. and Grondel, S. (2009) Applicability of Acoustic Noise Correlation for Structural Health Monitoring in Nondiffuse Field Conditions. *Applied Physics Letters*, **95**, Article ID: 094104. https://doi.org/10.1063/1.3200240

[16] Chehami, L., *et al*. (2014) Detection and Localization of a Defect in a Reverberant Plate Using Acoustic Field Correlation. *Journal of Applied Physics*, **115**, Article ID: 104901.

[17] Lobkis, O.I. and Weaver, R.L. (2001) On the Emergence of the Green's Function in the Correlations of Diffuse Field. *The Journal of the Acoustical Society of America*, **110**, 3011-3017. https://doi.org/10.1121/1.1417528

[18] Rickett, J. and Claerbout, J. (1999) Acoustic Daylight Imaging via Spectral Factorization: Helioseismology and Reservoir Monitoring. *The Leading Edge*, **18**, 957-960. https://doi.org/10.1190/1.1438420

[19] Sabra, K.G., Roux, P. and Kuperman, W.A. (2005) Emergence Rate of the Time-Domain Green's Function from the Ambient Noise Cross-Correlation Function. *The Journal of the Acoustical Society of America*, **118**, 3524-3531. https://doi.org/10.1121/1.2109059

[20] Nagayama, T., Abe, M., Fujino, Y. and Ikeda, K. (2005) Structural Identification of a Nonproportionally Damped System and Its Application to a Full-Scale Suspension Bridge. *Journal of Structural Engineering*, **131**, 1536-1545. https://doi.org/10.1061/(ASCE)0733-9445(2005)131:10(1536)

[21] Snieder, R. and Safak, E. (2006) Extracting the Building Response Using Seismic Interferometry: Theory and Application to the Millikan Library in Pasadena, California. *Bulletin of the Seismological Society of America*, **96**, 586-598. https://doi.org/10.1785/0120050109

[22] Draeger, C., Aime, J.-C. and Fink, M. (1999) One-Channel Time-Reversal in Chaotic Cavities: Experimental Results. *The Journal of the Acoustical Society of America*, **105**, 618-625. https://doi.org/10.1121/1.426252

[23] Benmeddour, F., Treyssde, F. and Laguerre, L. (2011) Numerical Modeling of Guided Wave Interaction with Non-Axisymmetric Cracks in Elastic Cylinders. *International Journal of Solids and Structures*, **48**, 764-774. https://doi.org/10.1016/j.ijsolstr.2010.11.013